Western Michigan University
ScholarWorks at WMU

Masters Theses

Graduate College

8-1969

Angular Correlation of Positron Annihilation Radiation in Damaged Nickel and Iron

Hsien Chen Huang
Western Michigan University

Follow this and additional works at: https://scholarworks.wmich.edu/masters_theses

 Part of the Physics Commons

Recommended Citation

Huang, Hsien Chen, "Angular Correlation of Positron Annihilation Radiation in Damaged Nickel and Iron" (1969). *Masters Theses*. 3044.
https://scholarworks.wmich.edu/masters_theses/3044

This Masters Thesis-Open Access is brought to you for free and open access by the Graduate College at ScholarWorks at WMU. It has been accepted for inclusion in Masters Theses by an authorized administrator of ScholarWorks at WMU. For more information, please contact wmu-scholarworks@wmich.edu.

ANGULAR CORRELATION OF POSITRON ANNIHILATION RADIATION IN DAMAGED NICKEL AND IRON

by

Hsien Chen Huang

A Thesis
Submitted to the
Faculty of the School of Graduate
Studies in partial fulfillment
of the
Degree of Master of Arts

Western Michigan University
Kalamazoo, Michigan
August 1969

Reproduced with permission of the copyright owner. Further reproduction prohibited without permission.

ACKNOWLEDGEMENTS

I wish to acknowledge my debt to Dr. John H. Kusmiss for illuminating and helpful discussions and assistance through this work. Also, I am grateful to Mr. Keith Mickle of the Physics Department electronics shop for the construction and maintenance of the automatic control unit used in the experiment.

Hsien Chen Huang

Reproduced with permission of the copyright owner. Further reproduction prohibited without permission.

MASTER'S THESIS M-2069

HUANG, Hsien Chen
ANGULAR CORRELATION OF POSITRON ANNIHILATION RADIATION IN DAMAGED NICKEL AND IRON.

Western Michigan University, M.A., 1969
Physics, solid state

University Microfilms, Inc., Ann Arbor, Michigan

Reproduced with permission of the copyright owner. Further reproduction prohibited without permission.

TABLE OF CONTENTS

Reproduced with permission of the copyright owner. Further reproduction prohibited without permission.

TABLE OF FIGURES

Reproduced with permission of the copyright owner. Further reproduction prohibited without permission.

CHAPTER I

INTRODUCTION

Since the first measurement by DeBenedetti et al. (1) on the angular distribution of positron annihilation radiation in gold, the technique of measuring the angular correlation of the gamma rays resulting from positron annihilation has been extensively used to investigate the momentum distribution of the electrons in solids, liquids, and semiconductors (2, 3, 4, 5, 6, 7) and to determine the shape of the Fermi surface of various metal single crystals (8, 9, 10).

The annihilation probability is directly proportional to the square of the Fourier transform of the positron-electron wave function product. In other words, the annihilation probability is determined by the electron density at the position of the positron.

According to the studies of earlier investigators, the angular correlation curves could be roughly divided into two classes. The curves of the first class are, by using the nearly-free-electron theory, those that appear to be very nearly inverted parabolas with a fairly sharp cut-off at an angle $\theta = \hbar k_{F/mc}$, where k_F is the wave

Reproduced with permission of the copyright owner. Further reproduction prohibited without permission.

vector corresponding to the Fermi surface, m is the electron mass, and c is the velocity of light. The alkali metals, alkaline earths, and aluminium belong to this class. Those of the second class, having a Gaussian shape, do not show any prominent Fermi cut-off and exhibit a wide distribution with high-momentum "tails". The noble metals, Ni, Fe, Zn, and Ga are examples of this class.

There is no doubt that it is necessary and important to take into account the interactions of the positron with the electron medium in attempting to understand the angular correlation measurements. After the measurements (11) of the angular distribution for polycrystalline samples were made, the possibility of measuring the electron momentum anisotropies by using oriented graphite was explored (12). The anisotropy of the Fermi surface in metals like Be and Li has also been demonstrated by Stewart et al. (13).

Some effects on the angular correlation curves produced by heating or melting metal specimens have been observed by Stewart et al. (3) and Gustafson (14). From these experiments, Stewart (7) and Majumdar (10) then described how the effective mass of the positron in metals could be determined.

Besides the angular correlation technique,

Reproduced with permission of the copyright owner. Further reproduction prohibited without permission.

determination of the annihilation lifetime, i.e., the inverse of the annihilation probability per unit time, of positrons in metals is another useful method for the analysis of their electronic properties. The lifetime measurements are done by the delayed-coincidence technique.

Forty years ago, Frenkel predicted that all solids should exhibit defects due to the effects of thermal fluctuations at sufficiently high temperatures. Therefore, the main cause of the temperature effects on the angular correlation curves might be due to the thermal generation of lattice vacancies. This point of view has been proposed after the dependence of the two-photon angular distributions and of positron lifetimes for several metals as a function of temperature has been studied (15, 16).

Recently, interest has been shown in using the annihilation lifetime and angular correlation techniques as tools in the investigation of the electronic properties in damaged solids. A large change in the observed two-gamma angular distribution from plastically deformed Ni, Fe-Ni alloys (17), Ta, Nb, Fe, and the solid solutions Fe + 0.63% Al and Fe + 1.08% Al (18) has been reported. The results obtained were qualitatively explained by the redistribution of s and d band

Reproduced with permission of the copyright owner. Further reproduction prohibited without permission.

electrons in the deformed areas of the crystal around dislocations. Very recently, Kim and Stewart (19) have measured the angular correlation obtained from quenched aluminium at liquid nitrogen temperature (78°K). They interpret their results in terms of the excess vacancies in quenched aluminium.

The purpose of the present work is to measure the shape of the momentum distributions in 2%, 4%, 8%, and 16% plastically deformed Ni and in high dose, medium dose, and low dose electron-irradiated Ni and Fe and to compare the results with those obtained from the same specimens after annealing at 100°C, 250°C, and 400°C.

The experimental results show higher annihilation rates in the central part of the angular correlation and narrowing of the rest of the curve. Experimental angular correlation curves and the discussion of the results are presented in Chapter IV. The effects of plastic deformation and electron irradiation on metals are discussed. For damaged metallic crystals so far investigated thoroughly by the transmission electron microscope, the point defects, i.e., vacancies and interstitials, have been found to be the most abundant defects.

The nature of positron annihilation with conduction electrons and with core electrons is discussed in Chapter II. The experimental setup and procedures are described

Reproduced with permission of the copyright owner. Further reproduction prohibited without permission.

in Chapter III. Experimental results are plotted as a function of the angular deviation from 180°, expressed in milliradians. The deviation is proportional to the z component of the momentum of the annihilating pair. Conclusions are presented in Chapter V.

Reproduced with permission of the copyright owner. Further reproduction prohibited without permission.

CHAPTER II

NATURE OF POSITRON ANNIHILATION IN METALS

Positron Thermalization

The question of positron thermalization must be considered because the thermalization time of a positron in a metal is pertinent to the interpretation of measurements of the angular correlation of annihilation radiation.

Because the short range interaction between a positron and an electron can be approximated by the exponentially screened Coulomb potential $-e^2r^{-1}\exp(-qr)$, where q is the screening parameter (20, 21), transitions occur from an initial positron-electron state with wave vector $\vec{k_+}$ and $\vec{k_-}$, respectively, to a final state with $\vec{k_+'}$ and $\vec{k_-'}$. An approximate integration of the rate of loss of energy by the positron shows that the positron energy falls to 4 eV in a negligible time, from 4 eV to 1 eV in about 3×10^{-15} sec, from 1 eV to 0.1 eV in about 2×10^{-13} sec, and from 0.1 eV to 0.025 eV in about 3×10^{-12} sec (20). Since positrons are observed (22) to annihilate in a metal with a lifetime, within 25 per cent, of about 1.5×10^{-10} sec, there

Reproduced with permission of the copyright owner. Further reproduction prohibited without permission.

seems to be no doubt that fast positrons in a metal are slowed down rapidly to thermal energies by collisions with the lattice and with electrons.

The Probability of Annihilation

As mentioned in the preceding section, a positron has reached thermal equilibrium with the lattice in a metal before it annihilates. We may therefore suppose that the positron-electron interacting system annihilates from its ground state ψ_o. We want to know the probability, $\rho(\vec{P})$, that the annihilating positron-electron pair has total momentum $\vec{P}$. It is known that $\rho(\vec{P})$ is given by the formula (23, 24)

$$\rho(\vec{P})=\frac{\alpha^2}{16\pi^3 m^2} < \psi_o | \sum_{\substack{\vec{k},\vec{k}' \\ \sigma,\sigma'}} \sigma\sigma' a^+_{\vec{k},\sigma} a_{\vec{k}',\sigma'} b^+_{\vec{p}-\vec{k},-\sigma} b_{\vec{p}-\vec{k},-\sigma'} | \psi_o >$$

where $\alpha = \frac{e^2}{\hbar c} \simeq \frac{1}{137}$, is the fine structure constant, m the electron mass, and $a^+_{\vec{k},\sigma}$, $a_{\vec{k},\sigma}$ are the creation and annihilation operators for electrons of momenta $\vec{k}$ and spin σ; similarly, $b^+_{\vec{k},\sigma}$, $b_{\vec{k},\sigma}$ are the corresponding operators for the positron. $\sigma = +1$ or -1 corresponds to spin up or down, respectively, along some fixed quantization axis. Therefore, the total annihilation rate is essentially determined by the expectation value $< \psi_o | \sum_{\substack{\vec{k},\vec{k}' \\ \sigma,\sigma'}} \sigma\sigma' a^+_{\vec{k},\sigma} a_{\vec{k},\sigma'} b^+_{\vec{p}-\vec{k},-\sigma} b_{\vec{p}-\vec{k}',-\sigma'} | \psi_o >$

Reproduced with permission of the copyright owner. Further reproduction prohibited without permission.

which is simply the electron density at the position of the positron, averaged over the positron position.

It was shown (23) that the Coulomb force on the positron should lead to a large enhancement of the annihilation rate.

Annihilation in a Free Electron Gas

Consider the metal to be treated as a set of ion-cores interacting with each other according to a Born-Mayer potential. These ion-cores are immersed in a sea of conduction electrons that are adequately described by the effective mass approximation. In Sommerfeld's quantum free-electron model (which is based on the assumption that the variations in potential across the atom are negligible), the wave function of an electron has the form $V^{-\frac{1}{2}} \exp(i\vec{k}\cdot\vec{r})$, where V is the volume of the metal. This is the expression for plane waves that are moving through space and carrying momentum as specified by $\vec{k}$. As discussed in the preceding section, let $\vec{P}$ be the center-of-mass momentum of an annihilating electron-positron pair. In the case of a degenerate electron gas, then,

Reproduced with permission of the copyright owner. Further reproduction prohibited without permission.

$$\rho(\vec{P}) = \frac{\alpha^2}{16\pi^2 m^2} \langle \psi_F \mid a^{+}_{\vec{p},-s}\, a_{\vec{p},-s} \mid \psi_F \rangle$$

$$= \frac{\alpha^2}{16\pi^2 m^2} \langle \bar{n}_{\vec{p},-s} \rangle_F$$

$$= \frac{\alpha^2}{16\pi^2 m^2} \begin{cases} 0\,, & P > P_F \\ 1\,, & P \leq P_F \end{cases}$$

where ψ_F is the ground state wave-function for the system of electrons and P_F is the Fermi momentum of the electrons. At $T = 0°K$, $\rho(\vec{P})$ is constant inside the Fermi surface.

Hence the probability that the annihilation will produce two quanta having the Z component of momentum P_Z, which is experimentally measured, is

$$\rho(P_Z) = \int_{-\infty}^{\infty} \int_{-\infty}^{\infty} \sum_{\text{electrons}} \rho(\vec{P})\, dP_X\, dP_Y$$

$$= \frac{\alpha^2}{16\pi^2 m^2} (P_F^2 - P_Z^2)$$

Therefore the angular correlation apparatus measures a counting rate

$$N(\theta) \propto (P_F^2 - P_Z^2) \propto (\theta_F^2 - \theta^2)$$

where $\theta = P_Z/mc$, $\theta_F = P_F/mc$. The expected angular distribution for the free electron gas is then an inverted parabola which is symmetrical about $\theta \simeq 0°$ and which goes to zero at $\pm \theta_F$, the Fermi cut-off angle.

Reproduced with permission of the copyright owner. Further reproduction prohibited without permission.

$\rho(P_z)$, therefore, is proportional to the area of a section of the Fermi surface normal to the direction of P_z. Thus the angular correlation may give information about the Fermi surface.

However, when the potential energy of an electron is modulated by the periodicity within a crystal, the wave functions which are valid solutions of Schrodinger's equation are the Bloch state functions

$$\psi_-(\vec{r}) = V^{-\frac{1}{2}} U_k(\vec{r})\, e^{i\vec{k}\cdot\vec{r}}$$

so that $\vec{P}$ and $\vec{k}$ are not equivalent anymore. Consider a positron in the state $\psi_+(\vec{r}) = V^{-\frac{1}{2}} \psi_+(\vec{r})$. The contribution to the momentum distribution due to all occupied states in a given band is proportional to the square of the absolute value of the Fourier transform of the positron-electron wave function product

$$\sum_k \left| \int \psi_+^*(\vec{r})\, U_k(\vec{r}) e^{i(\vec{k}-\vec{p})\cdot\vec{r}}\, d^3\vec{r} \right|^2$$

where the functions $\psi_+(\vec{r})$ and $U_k(\vec{r})$ have the periodicity of the lattice, and $\vec{r}$ is the position in the crystal.

Annihilation with Core Electrons

It seems reasonable that the annihilations taking place with core electrons become more appreciable in heavy elements. The bound electrons are much more

Reproduced with permission of the copyright owner. Further reproduction prohibited without permission.

numerous than the conduction electrons in heavy elements. Therefore, they contribute appreciably to the angular correlation distribution.

By using the tight-binding approximation, Berko and Plaskett (9) were able to derive the probability distribution of the annihilating positron-core electron pairs having momentum $\vec{P}$ as

$$\rho_{n\ell}(\vec{P}) = \frac{\alpha^3}{4\pi^2} \sum_{m=-\ell}^{\ell} \left| \int_V \psi_+^*(\vec{r})\, \psi_{n\ell m}(\vec{r}) e^{-i\vec{p}\cdot\vec{r}}\, d^3\vec{r} \right|^2$$

where $\psi_{n\ell m}$ is a Hartree-Fock atomic function and n, ℓ, and m describe the atomic state. This result, combined with a model (25) for the positron wave function based on a Wigner-Seitz calculation, provides a reasonable description of the annihilation of positrons with core electrons in metals.

Reproduced with permission of the copyright owner. Further reproduction prohibited without permission.

CHAPTER III

EXPERIMENTAL SETUP AND PROCEDURES

Mechanical Apparatus

The physical arrangement of the experimental apparatus is shown in Fig. I. The experimental setup consisted of a positron source, shielded by lead, a target holder, a stationary and a moving detector and associated collimators mounted on a steel frame. The positron source was 2.5 mC of Na^{22} deposited on a stainless steel disc and was suspended from a threaded steel rod which allowed it to be moved away from or toward the sample as desired. The source of positrons was mounted above the specimen, which was threaded also so it could be used to adjust the sample height. The radioactive source was shielded by an 8 x 8 x 8-in. cube of 2-in. thick lead bricks to prevent the gamma-ray detectors from seeing the radioactive source or annihilations in the sample platform.

Twelve inches from either side of the source chamber, two 4 x 0.5-in. horizontal collimators made of 2-in. thick lead bricks were located. Gamma rays produced by annihilations in the sample were detected by two

Reproduced with permission of the copyright owner. Further reproduction prohibited without permission.

Reproduced with permission of the copyright owner. Further reproduction prohibited without permission.

1. NaI (Tℓ) Crystal Photo-mult. Pre-Amp.
2. Detector Chamber
3. Rough Collimating Lead Bricks
4. Source Chamber
5. Source Na^{22}
6. Sample
7. Drive Motor

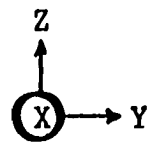

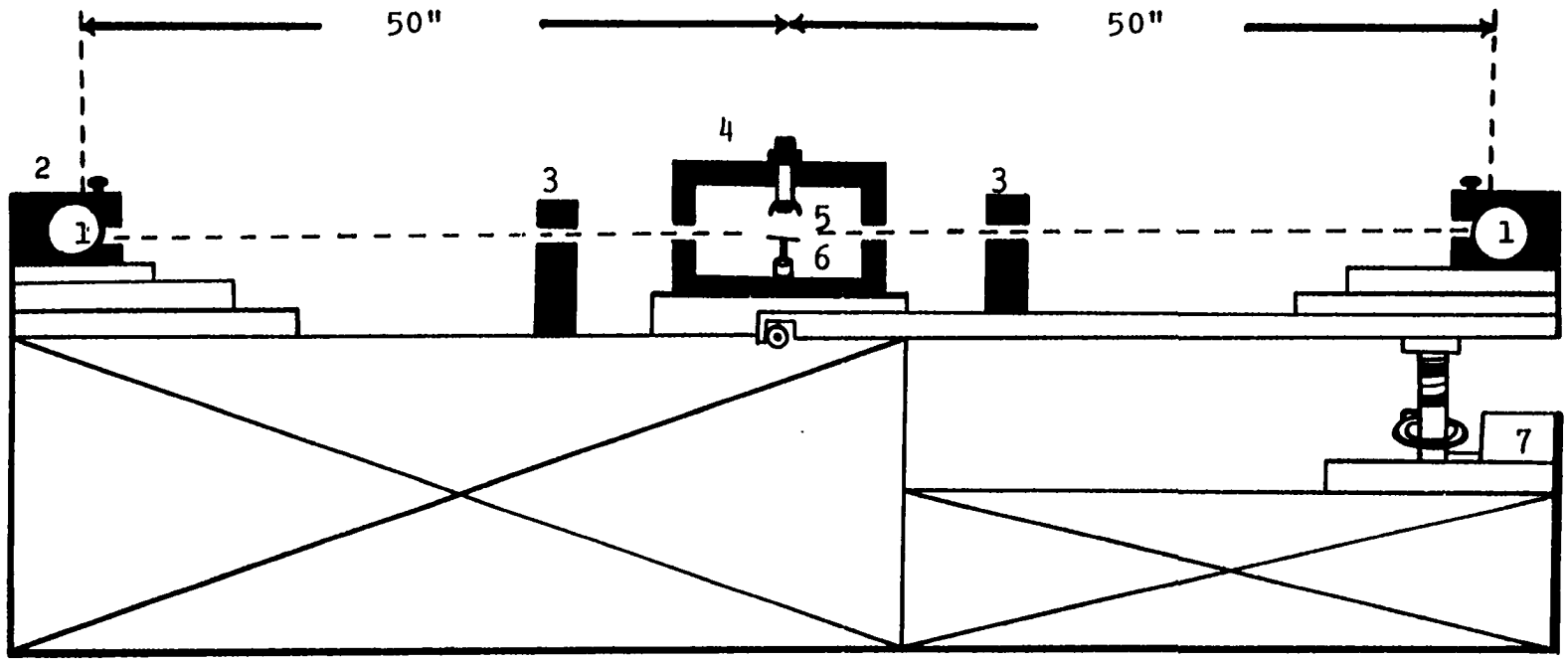

Fig. I. Experimental Setup

2 x 6-in. Harshaw NaI(Tl) crystals. The NaI(Tl) crystals were optically coupled by Dow Corning QC-2-0057 silicone grease to RCA 6342A photomultiplier tubes. The detectors were located at equal distances of 50 inches from the sample. Inorganic crystals have an excellent efficiency for gamma ray capture, due to their high density. In front of each of the detectors, a pair of lead slabs, each 12 x 0.5 x 3-in., are placed one above the other with a 0.05-in. opening to provide more collimation. These openings were adjusted by a bolt on the top lead brick. In addition, three large bolts placed at the vertices of a triangle were used to adjust the tilt of the detector platform to make sure of the alignment of these openings with the source chamber slits. These lead collimating slits provided the apparatus with an angular resolution of one milliradian.

Additional shielding with 2-in. thick lead bricks surrounding the detectors also served to reduce the accidental background.

In this arrangement, the source chamber and one of the detectors remained stationary while the other detector platform was moved up or down mechanically, in steps of one milliradian, by a threaded steel shaft. A 115 V.D.C. Bodine Motor rated at 1/20 horsepower was used to rotate the threaded steel shaft upon receiving a signal

Reproduced with permission of the copyright owner. Further reproduction prohibited without permission.

from the control circuit.

Electronic System

The Electronic System consisted of a fast coincidence system obtained commercially from Hamner Electronics of Princeton, New Jersey, and the control circuit which governed the automatic operation of the angular correlation equipment. A block diagram of the electronic system used for angular correlation measurements is given in Fig. II.

The resolving time of the Hamner NL-16 coincidence module can be adjusted from 5 nsec to 150 nsec. First of all, when the 511 keV annihilation gamma rays are collimated and then enter the detectors, they will interact either by the photo-electric effect or the Compton effect. In the former case it is reasonable to assume that the ejected photoelectron will deposit all its energy in the scintillator; in the Compton effect, however, the scattered photons may or may not be captured in the scintillator, depending on the size and geometry of the detector. The light output of a NaI(Tl) crystal is a long pulse about 0.2 nsec in duration.

The electrical outputs of the photomultipliers are then fed to separate Hamner NB-12 preamplifiers. The preamplified pulses propagate down equal lengths of

Reproduced with permission of the copyright owner. Further reproduction prohibited without permission.

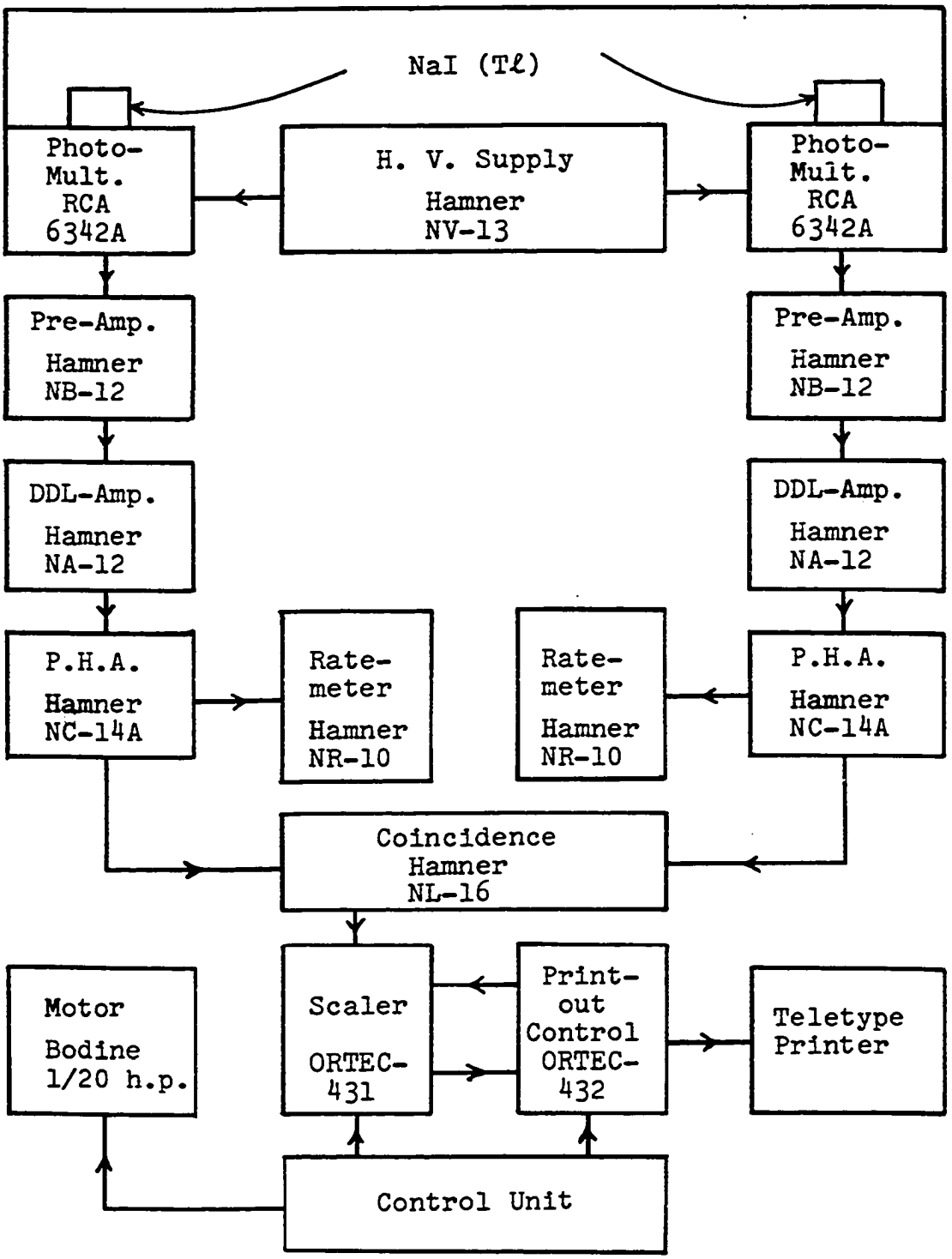

Fig. II. A Block Diagram of Electronic System used for Angular Correlation Measurements

Reproduced with permission of the copyright owner. Further reproduction prohibited without permission.

coaxial cable and then are fed into Hamner NA-12 double delay line amplifiers followed by Hamner NC-14A low jitter pulse height analyzers. The single-channel analyzer consists essentially of two triggers where the threshold of trigger A is always set higher than the threshold of B by an amount Δ E. If then an input signal passes through trigger B, which is set at threshold E, but not through A, set at E + Δ E, an output is obtained. E and Δ E can be manually adjusted. The photomultipliers were operated at a voltage of 700 volts from the NV-13 high voltage power supply. A Hamner NH-84A power supply was used to supply all other Hamner equipment.

The outputs of the pulse height analyzers are monitored by Hamner NR-10 linear ratemeters and also fed to a Hamner NL-16 fast ramp coincidence circuit. The coincidence outputs are then fed into ORTEC-431 scaler.

After the desired counting time at each position of the moveable detector elapses, the accumulated number of annihilations from the scaler is then printed out by the Teletype page printer.

The control circuit consists of an electronic timer which works with several relays. One can set a timing interval of approximately 1 minute, 2 minutes, 5 minutes, 10 minutes, or 15 minutes. It was decided to use

Reproduced with permission of the copyright owner. Further reproduction prohibited without permission.

10-minute counting intervals. Starting from the lowest position of the detector platform the drive motor is switched off and the scaler begins to count for ten minutes. At the end of the preset time period the scaler stops counting and the total count is printed out by the ORTEC-432 print-out control. The scaler is then reset to zero. At this time the drive motor is switched on and the scaler is prevented from counting until a microswitch removes the power from the motor. The scaler starts to count again for the next detector position. Once the detector platform reaches the desired highest position, it actuates another microswitch which reverses the motor until a microswitch at the bottom limit of its motion reverses it again. Repetitive sweeps of the entire angular range were employed in this manner to minimize any fluctuations in the electronics that might occur during the rather long time (about 5 days) required to get sufficient data.

Two Hamner NR-10 linear ratemeters, which monitor the count rates of the separate channels, are useful in checking the operation of the electronic equipment as well as the positioning of the source, sample, and detector slits.

Reproduced with permission of the copyright owner. Further reproduction prohibited without permission.

Positron Source and the Sample

From the level diagram of Na^{22} decay, we know that positrons are emitted according to

$$_{11}Na^{22} \longrightarrow {}_{10}Ne^{22*} + e^{+} + \nu .$$

The pulse-height spectrum from Na^{22} shows a peak at 0.511 MeV from annihilation radiation; the smaller peak at 1.277 MeV is due to the de-excitation of Ne^{22*} .

The advantages of Na^{22} are a long half-life (2.6 years) and a 1.277-MeV gamma ray coincident with the positron emission which can be used as a trigger pulse for positron lifetime experiments.

All metal samples were 25 x 3-mm., 0.5 mm. thick rectangular plates. The damaged samples (high dose, medium dose, and low dose electron-irradiated Ni) and Fe; 2%, 4%, 8%, and 16% plastically deformed Ni; and the Ni and Fe annealed at 1150°C were prepared for us at Brookhaven National Laboratory. The deformation was produced by rolling at room temperature. These samples were originally at least 99.95% pure before the damage.

High dose, medium dose, and low dose irradiation-damaged samples were bombarded by electrons with energies in the neighborhood of two MeV, respectively. Ni samples annealed at 100°C and 250°C were prepared by heating the high dose electron-irradiated and the 16% plastically

Reproduced with permission of the copyright owner. Further reproduction prohibited without permission.

deformed samples up to 100°C or 250°C in an oven for about an hour and then cooling down to room temperature.

Angular Correlation Technique

As was mentioned in Chapter II, positrons entering a metal will make many collisions and end up in thermal equilibrium with the lattice in a time short compared to their lifetime. Annihilation from the singlet spin state ($S = 0$, the electron and positron spins are antiparallel) occurs by two quantum annihilation. Annihilation from the triplet state ($S = 1$, the electron and positron spins are parallel) with the emission of three gamma rays can also occur, but the probability of three quantum annihilation relative to two quantum annihilation is of the order of the fine structure constant ($\alpha = 1/137$), or actually about 1/370 for annihilation of a free positron with a free electron.

Consider a positron which annihilates with an electron via two photons. Let one of the photons (call it photon "1") make an angle ϕ with respect to the momentum of the electron being annihilated, assuming the positron to be at rest as shown in Fig. III. If the momentum mv of the electron were zero, conservation of momentum would require the two photon directions to be antiparallel, each photon having a momentum $p = mc$.

Reproduced with permission of the copyright owner. Further reproduction prohibited without permission.

Reproduced with permission of the copyright owner. Further reproduction prohibited without permission.

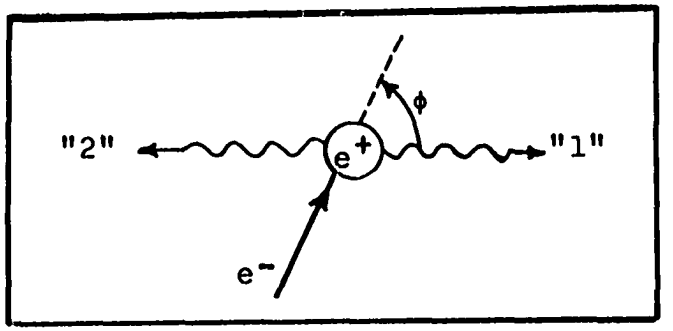

Fig. III. Conservation of Momentum in Two-Gamma Annihilation

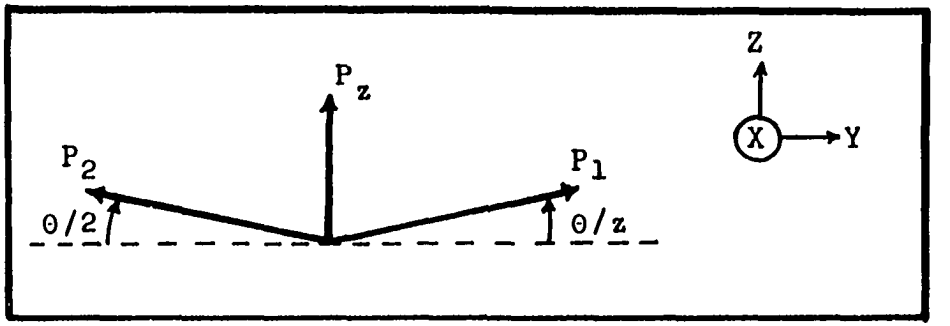

Fig. IV. Momentum Diagram

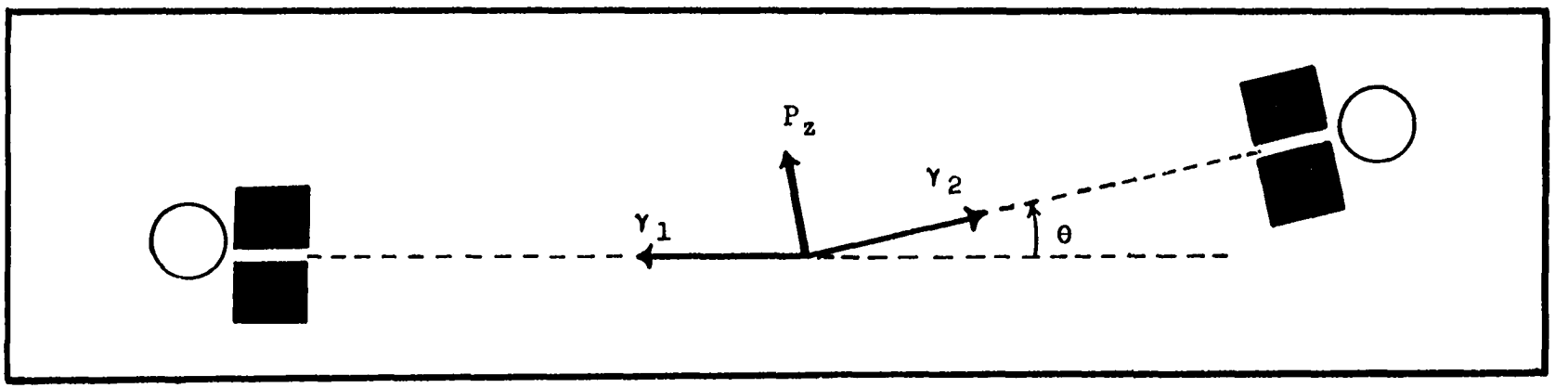

Fig. V. Detector Arrangement

For $mv \neq 0$, there is a momentum $\Delta p = mv \sin\phi$, perpendicular to the direction of photon "1" which must be carried by the other photon. Thus to first order in v/c, the photon directions deviate from collinearity by the angle

$$\theta = \frac{\Delta P}{P} = \frac{mv \sin\phi}{mc} = \frac{P_z}{mc} .$$

Since the probability of a given angular separation depends only on the probability of an electron having the appropriate momentum in the direction bisecting the angle between the photon momenta, the direction of $\Delta\vec{p}$ makes a convenient choice for the Z-axis. Hence, we write $P^2 = P_{XY}^{\ 2} + P_Z^{\ 2}$, where P_{XY} is in the plane normal to $\vec{P}_Z$.

Because the long collimating slits in the geometrical arrangement of the apparatus are parallel to the X-direction, the X component of momentum is essentially integrated over. The Y component of momentum is also integrated over because the detector is set to accept gamma-rays having energies in a range of several keV . The momentum diagram is shown in Fig. IV. Therefore, the angular correlation setup is used to obtain a measure of $\rho(P_Z)$, the probability distribution of the Z component of the momentum of the annihilating pair. The angular distribution thus measured is

$$N_Z(\theta) \propto \int\int \rho(P_X\ P_Y\ mc\theta)\ dP_X\ dP_Y ,$$

Reproduced with permission of the copyright owner. Further reproduction prohibited without permission.

the number of coincident gamma-ray pairs at various angles of the detector, as shown in Fig. V. The angle θ is changed by moving the detector along the arc of a circle with the sample at the center and the detector at the left remaining fixed.

With the 2.5 mC Na^{22} source, about twenty thousand coincidences could be obtained in five days at 0° with roughly one milliradian resolution. Data were taken in steps of one milliradian, recycling twenty times over the preset number of thirty-eight positions. It was decided to tip the sample a little bit to minimize absorption of the gamma rays in the sample, so that the real resolution is slightly larger than one milliradian.

The resolving time of the coincidence equipment was set at 30 nsec for this experiment. The number of accidental coincidences is equal to $2\tau N_1 N_2$, where 2τ is the resolving time of the coincidence equipment and N_1 and N_2 are the individual count rates of each channel. The accidental coincidence rate was calculated to be 5 counts per ten minutes. At the tails of the angular distribution curves about 10 counts per ten-minute time interval were counted, which did not exceed in any of the runs one per cent of the counting rate at the peak of the curve, which was approximately 1,000 counts in ten minutes.

Reproduced with permission of the copyright owner. Further reproduction prohibited without permission.

The raw data, the coincidence counting rate at each angle of the detector, which is printed out automatically by the Teletype printer on a strip of paper, is originally in the form of thirty-eight sets of numbers. One must then add up all twenty of the data numbers corresponding to the same angular position. The result is a series of thirty-eight numbers, each of which is the sum of twenty other numbers.

Next, these thirty-eight numbers are punched on thirty-eight cards, one for each number, and fed into an IBM 1620 Computer with a Fortran program which has been written to analyze the data. The centroid of the angular distribution is calculated by finding the largest counting rate and using the formula (6)

$$N_{center} = \frac{S_+ + S_-}{2(S_- - S_+)}$$

where

$$S_+ = \sum_{i=1}^{n} Y_i - Y_o - \sum_{i=1}^{n-1} Y_{-i}$$

$$S_- = \sum_{i=1}^{n-1} Y_i + Y_o - \sum_{i=1}^{n} Y_{-i}$$

Y_o is the number of counts in the central point of the angular distribution, Y_i , and Y_{-i} are the numbers of counts in the i^{th} points to either side of the center. Finally, Simpson's rule is used to approximate the area

Reproduced with permission of the copyright owner. Further reproduction prohibited without permission.

under the angular correlation curve. All curves have been normalized to an area of 10^5 .

The normalized data are then plotted as a function of θ , the angular separation of the annihilation gamma rays. Because $N(\theta)$ is symmetrical, all the data have been shown on one side of the line of symmetry, $\theta = 0°$. All the experiments were performed at room temperature.

The normalized angular correlation curves will be presented in the next chapter.

Reproduced with permission of the copyright owner. Further reproduction prohibited without permission.

CHAPTER IV

ANGULAR CORRELATION RESULTS AND DISCUSSION

Interpretation of the Angular Correlation Curves

The angular correlation of two-photon annihilation radiation from positrons annihilating in 2%, 4%, 8%, and 16% plastically deformed nickel and in electron-irradiated nickel and iron has been studied. Figures VI, VII, and VIII are comparisons of the normalized angular correlation curves from the high-dose electron-irradiated iron and iron annealed 1150°C, from the high-dose irradiated nickel and nickel annealed at 1150°C, and from the high-dose irradiated nickel and nickel annealed at 400°C, respectively. Figures IX, X, XI, and XII are comparisons of the angular correlation curves from the 16% plastically deformed nickel and nickel annealed at 1150°C, from the 16% plastically deformed nickel and nickel annealed at 400°C, from the 4% and 8% plastically deformed nickel, and from the high-dose irradiated and the 16% plastically deformed nickel, respectively. Finally, Fig. XIII is a comparison of the normalized angular correlation curves from two nickel samples annealed at 1150°C. The size of circles and triangles

Reproduced with permission of the copyright owner. Further reproduction prohibited without permission.

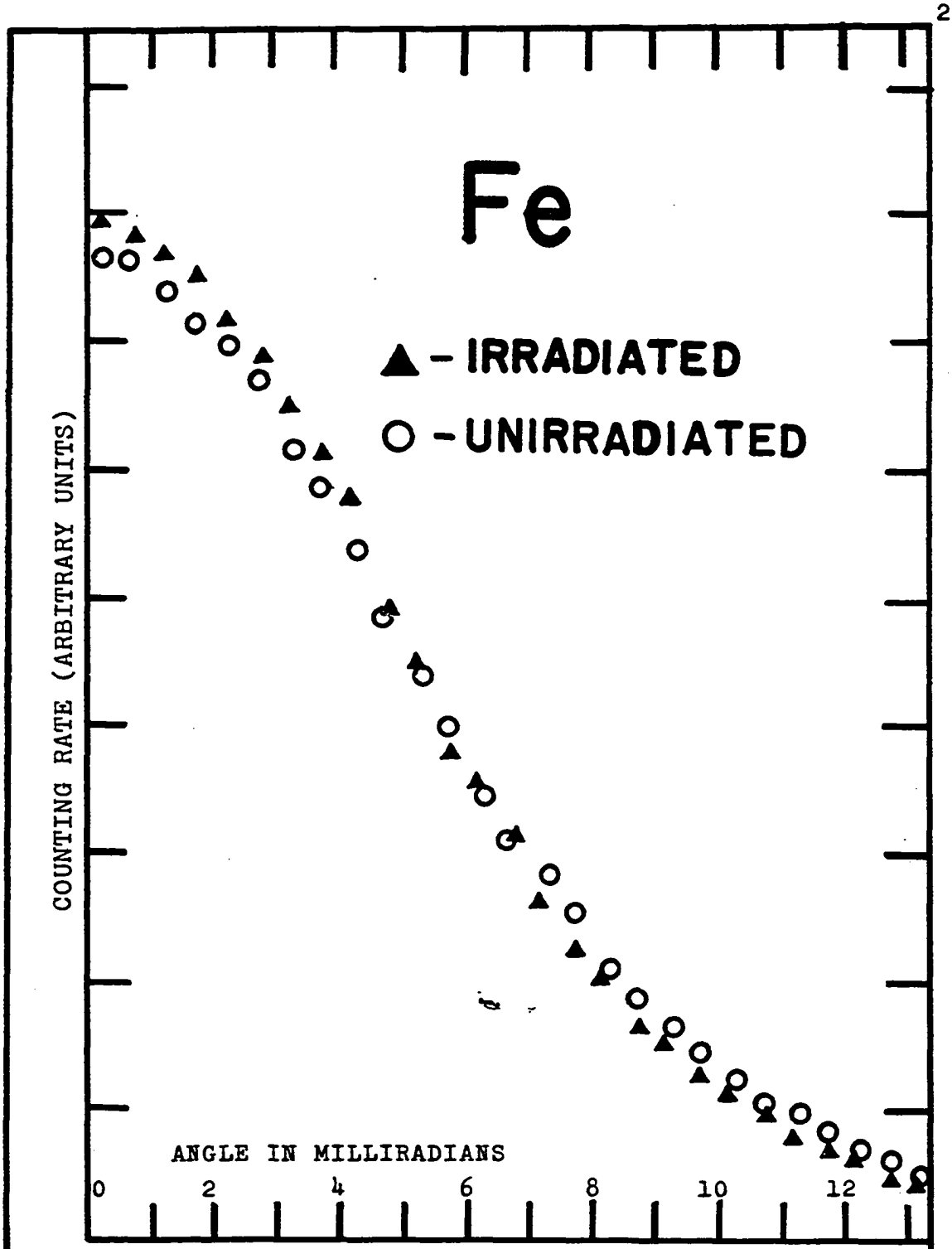

Fig. VI. Angular Correlation Curves for High-dose Electron-irradiated Fe and Fe Annealed (unirradiated) at 1150°C

Reproduced with permission of the copyright owner. Further reproduction prohibited without permission.

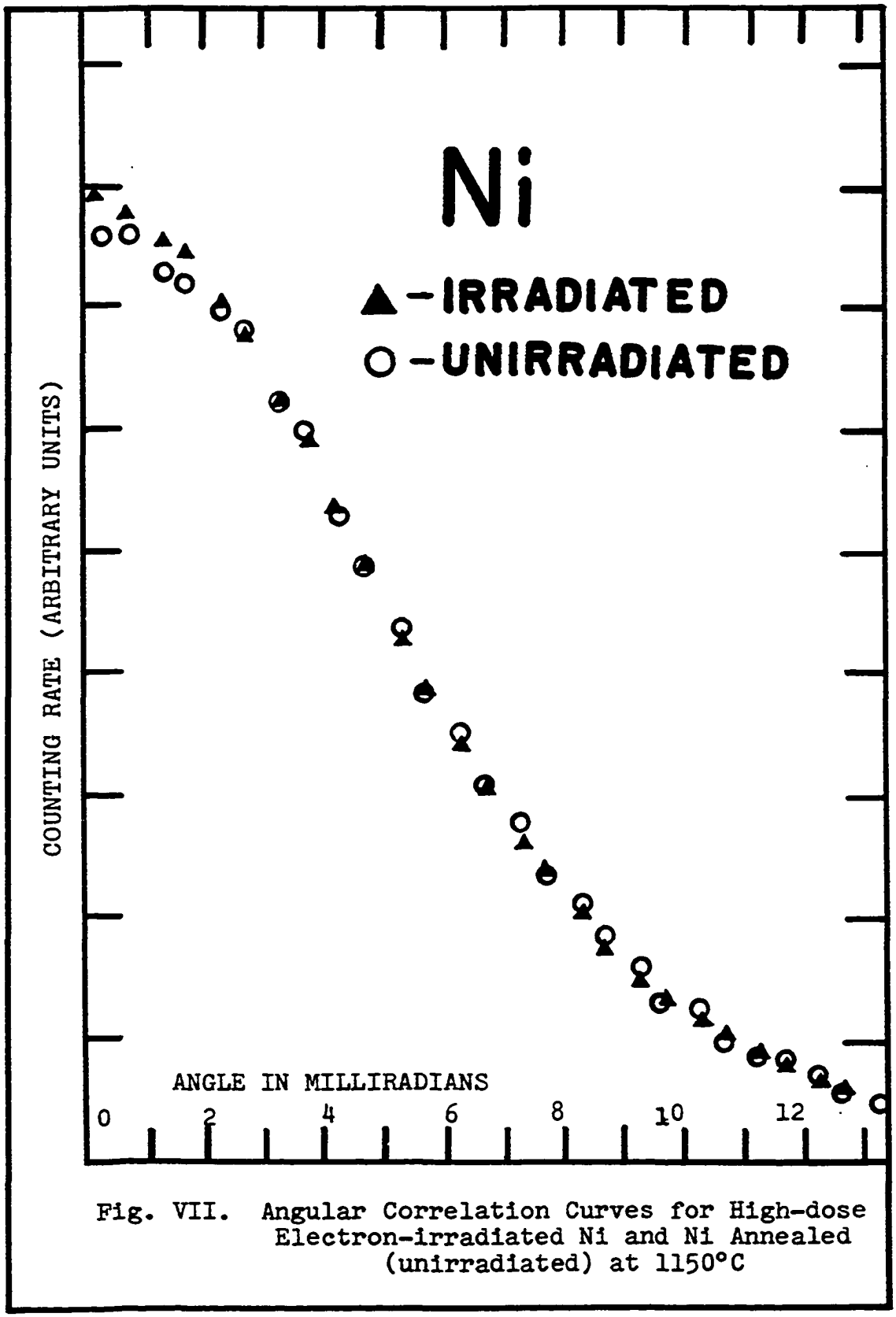

Fig. VII. Angular Correlation Curves for High-dose Electron-irradiated Ni and Ni Annealed (unirradiated) at 1150°C

Reproduced with permission of the copyright owner. Further reproduction prohibited without permission.

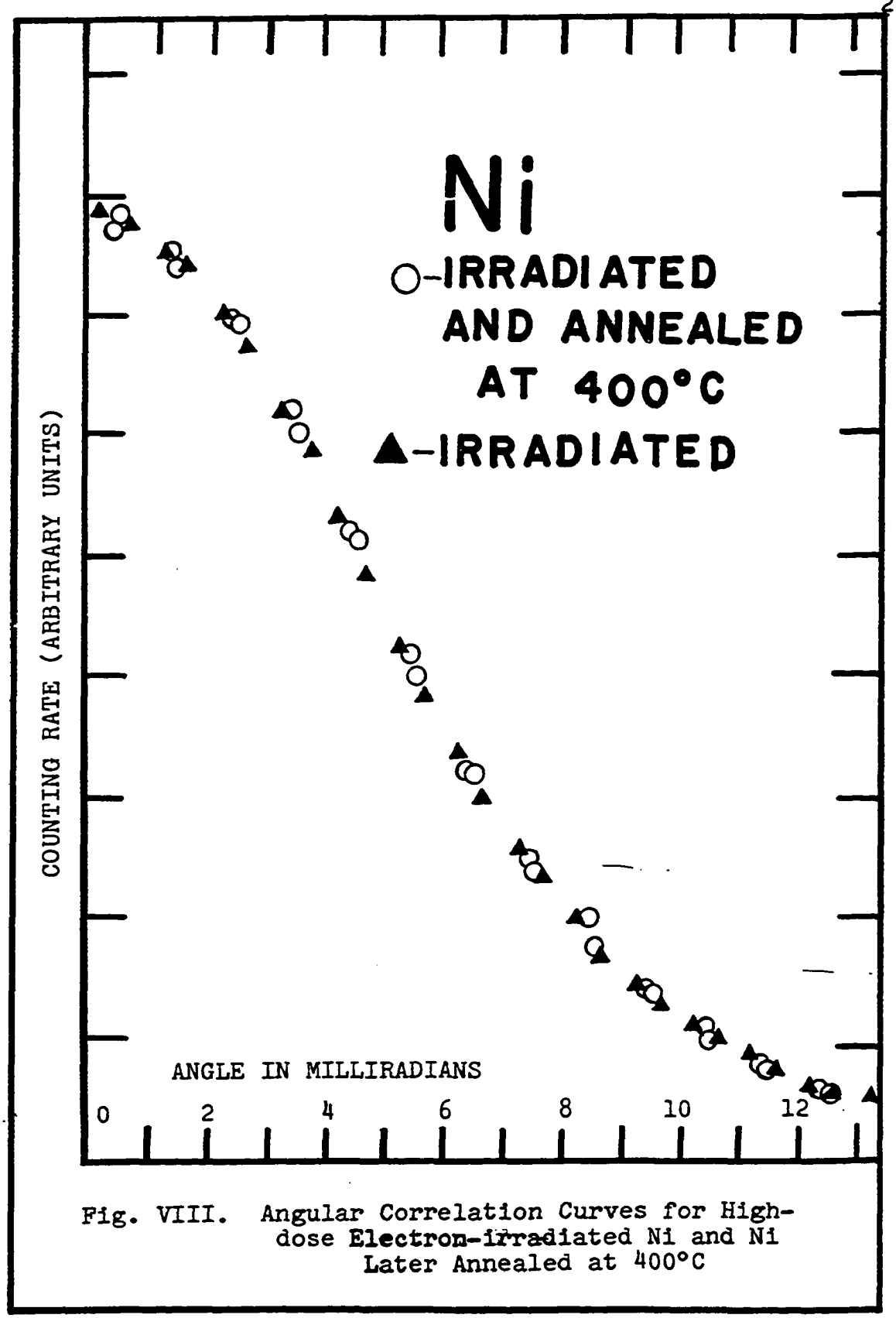

Fig. VIII. Angular Correlation Curves for High-dose Electron-irradiated Ni and Ni Later Annealed at 400°C

Reproduced with permission of the copyright owner. Further reproduction prohibited without permission.

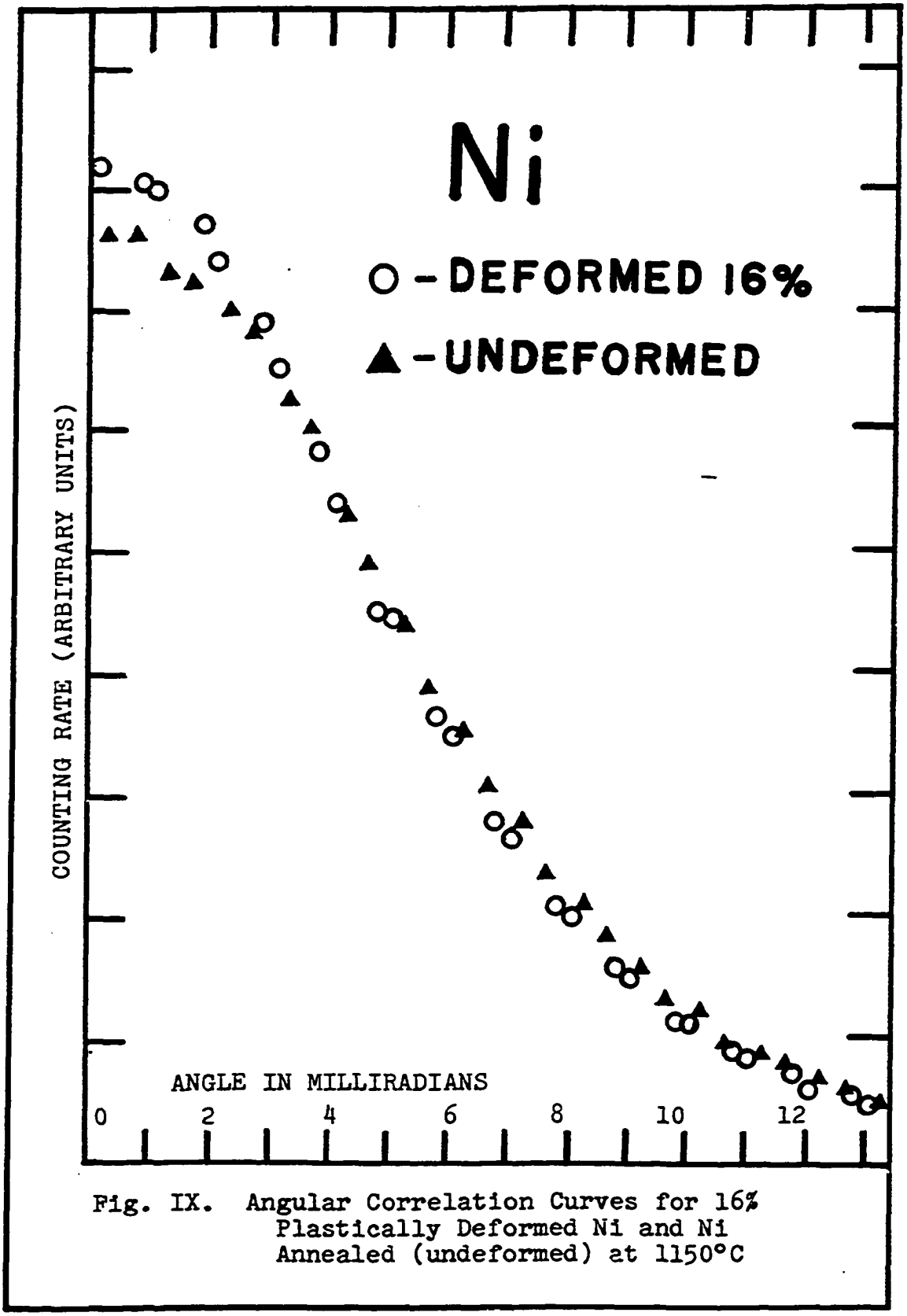

Fig. IX. Angular Correlation Curves for 16% Plastically Deformed Ni and Ni Annealed (undeformed) at 1150°C

Reproduced with permission of the copyright owner. Further reproduction prohibited without permission.

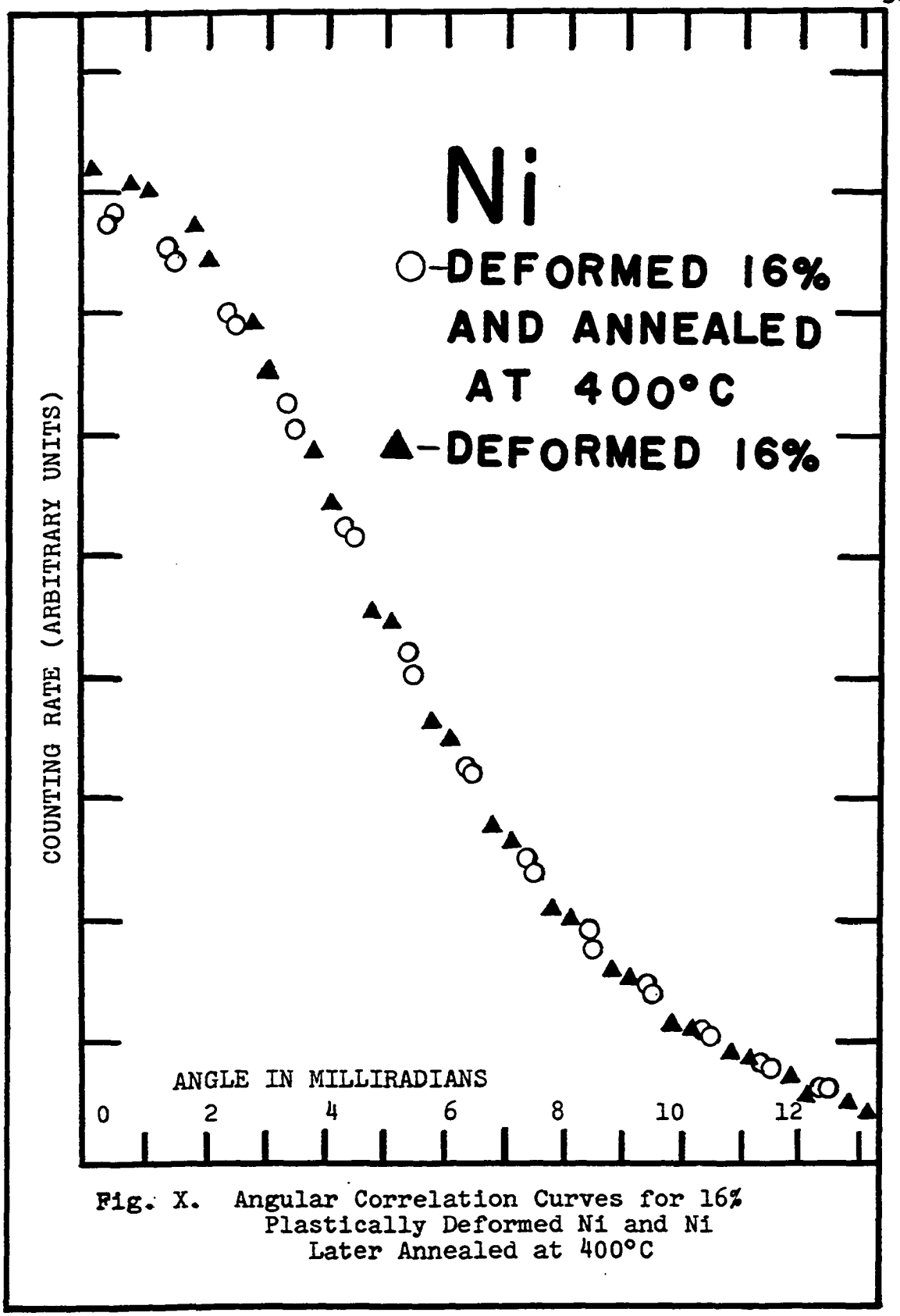

Fig. X. Angular Correlation Curves for 16% Plastically Deformed Ni and Ni Later Annealed at 400°C

Reproduced with permission of the copyright owner. Further reproduction prohibited without permission.

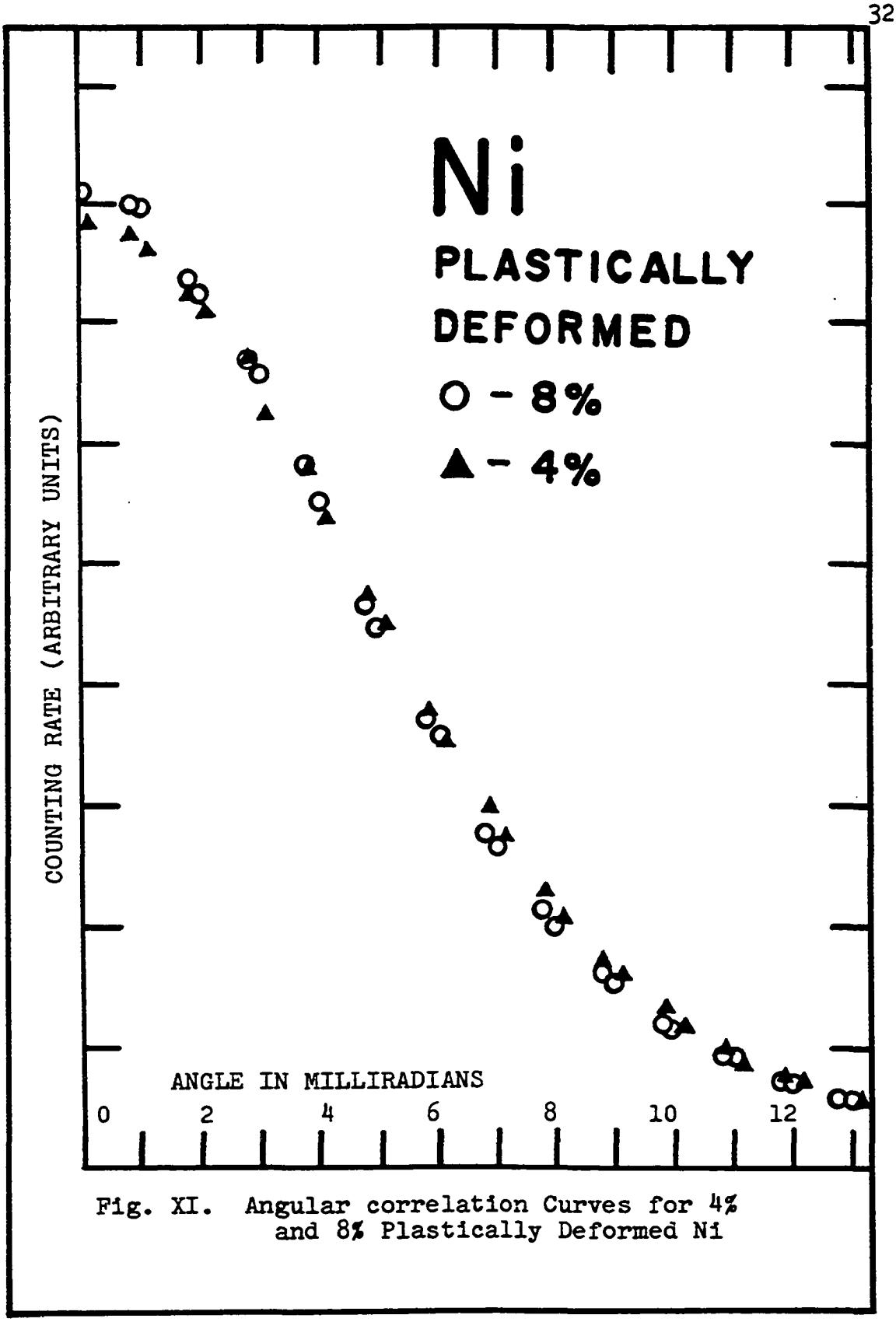

Fig. XI. Angular correlation Curves for 4% and 8% Plastically Deformed Ni

Reproduced with permission of the copyright owner. Further reproduction prohibited without permission.

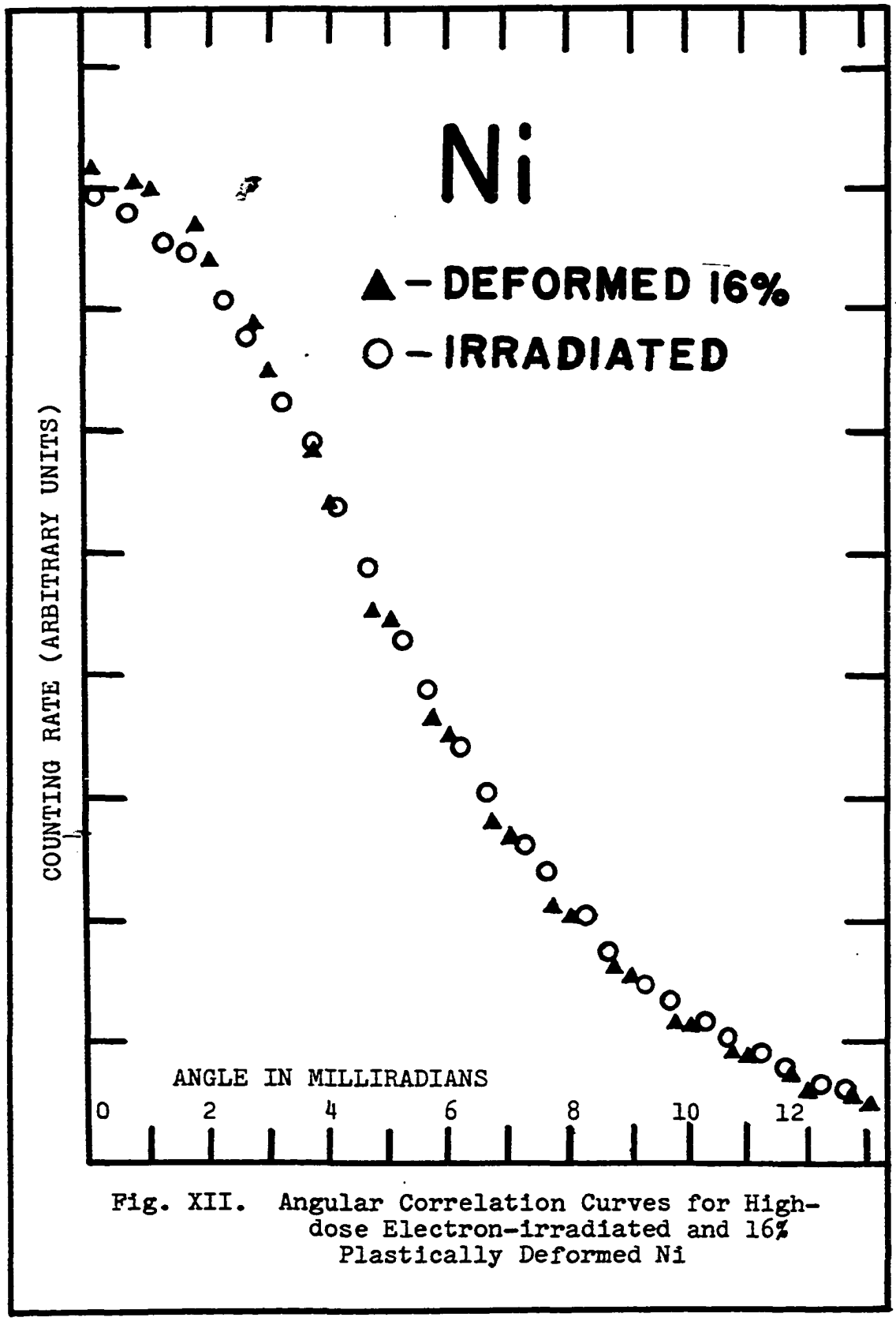

Fig. XII. Angular Correlation Curves for High-dose Electron-irradiated and 16% Plastically Deformed Ni

Reproduced with permission of the copyright owner. Further reproduction prohibited without permission.

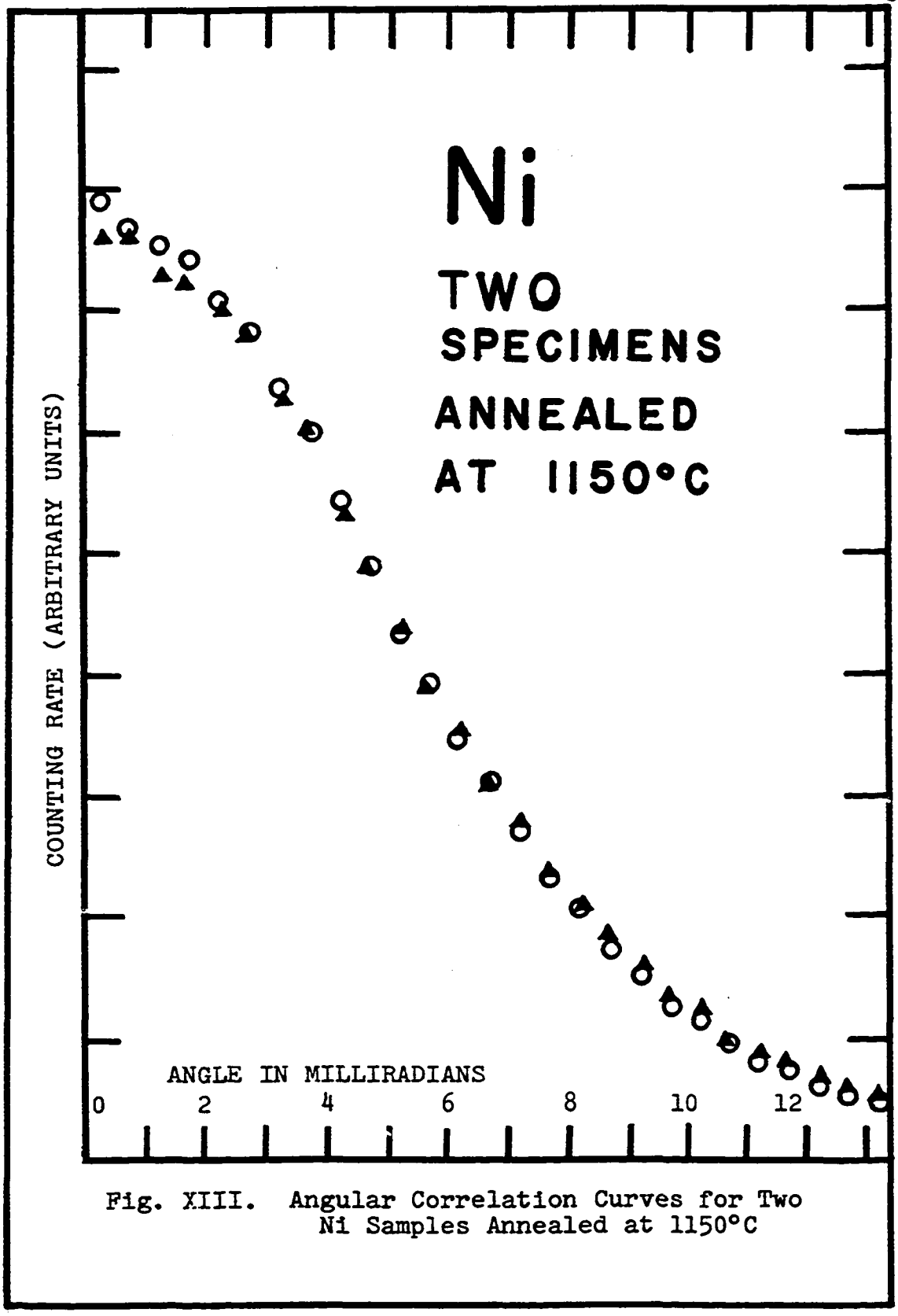

Fig. XIII. Angular Correlation Curves for Two Ni Samples Annealed at 1150°C

Reproduced with permission of the copyright owner. Further reproduction prohibited without permission.

in all experimental curves is roughly two standard deviations from the mean at the peak positions.

First of all, by looking at Fig. VI, Fig. VII, and Fig. IX, one can see a smooth and broad curve from the nickel and iron annealed (undamaged) at 1150°C, respectively.

In a review of band theory of Ni ($1s^2 2s^2 2p^6 3s^2 3p^6 3d^8 4s^2$) and Fe ($1s^2 2s^2 2p^6 3s^2 3p^6 3d^6 4s^2$), we may assume certainly that Fe resembles Ni in having partly filled d bands and s-p bands. It is well known that the density of levels in the d band is higher than that in the s-p band. In transition metals, where the atomic cores are close to each other, the large momenta in the counting rate are more pronounced, suggesting annihilation with core electrons, particularly 3d electrons. Contributions to the high momentum part of the counting rate can also be from the 3p and 3s electrons as well as the conduction electrons (the ion-lattice potential introduces higher momentum components in the conduction-electron wave function).

As mentioned before, the annihilation of positrons with core electrons in metals may be understood on the basis of the model for the positron wave function based on a Wigner-Seitz calculation. There seems to be no doubt that the contribution to the central part of the

Reproduced with permission of the copyright owner. Further reproduction prohibited without permission.

angular distribution from the iron and the nickel annealed at 1150°C was due to the annihilations with the conduction electrons, which to a first approximation may be considered free.

Changes in the experimental results as shown in Fig. VI, Fig. VII, and Fig. VIII, Fig. IX, and Fig. X, point out two interesting effects: (a) an increase of the central part of the curve, and (b) a narrowing of the rest of the curve for the damaged specimen.

Electron irradiation and plastic deformation of metals produces vacancies (more details are discussed in the next two sections). Transmission electron microscope studies of thin metal films and the measurements of increasing electrical resistivity in damaged metals support this.

A vacancy site in the metal is one missing an ion. Because of the lack of a positive ion at a vacancy site, the created vacancies could be considered as excess negative charges. A positron will be more attracted to the site than to lattice sites at which there are no vacancies. Therefore, the effect (a), the higher annihilation rate in the region of small angles on the experimental angular distribution of quanta for the plastically deformed nickel and the electron-irradiated nickel and iron, is more likely due to the 4s and 3d

Reproduced with permission of the copyright owner. Further reproduction prohibited without permission.

electrons. In attempting to explain the effect (b), the creation of vacancies, which decreases the density of electrons at vacancy lattice sites, is responsible for the narrowing of the angular correlation curves from the damaged iron and nickel at large angles.

In the case of metals, the damaged-induced defects do not change the number of charge carriers; the electrical conductivity change in damaged metals is due to a change in electron mobility. In other words, defects become an important factor limiting the mean free path of electrons and contribute to the resistivity.

A comparison of the angular correlation curve for the 2% plastically deformed nickel has been made. We found no significant difference between the shape of the angular correlation curves from the 2% and the 4%, those of the 8% and the 16%, and those of the 16% and the 45% (26) plastically deformed nickel. However, there is an apparent difference between the shapes of the angular correlation curves from the 4% and the 8% plastically deformed nickel, as can be seen in Fig. XI. Therefore, perhaps the concentration of vacancies in the plastically deformed nickel could be proportional to the deformation up to 8% and then saturate the effect on angular distributions.

When 16% plastically deformed nickel were annealed

Reproduced with permission of the copyright owner. Further reproduction prohibited without permission.

at 400°C in oven for one hour, the recovery of defects was nearly complete, as can be seen in Fig. X. Angular correlation curves for the high-dose irradiated and the 16% plastically deformed nickel annealed near 100°C and 250°C have also been obtained. We found no partial recovery for annealing at 100°C and 250°C. These data are in agreement with the electrical resistivity recovery data on electron-bombarded nickel reported by Sosin et al. (27). They indicated that final recovery due to vacancy migration occurred near 270°C. Cottrell (28) stated that all damage due to either irradiation or plastic deformation in nickel should anneal out below 400°C.

The angular correlation curves resulting from the high-dose (1.42×10^{19} electrons/cm^2), medium-dose (1.38×10^{18} electrons/cm^2), and low-dose (6.45×10^{17} electrons/cm^2) irradiated nickel have been measured also. The specimens were irradiated at liquid argon temperature (93°K). We find no difference between them. Also, the angular correlation curves for high-dose irradiated nickel and the same specimen later annealed at 400°C for one hour are the same as shown in Fig. VIII. The reason why they are the same is most likely that most of the vacancies produced by the electron bombardment were somehow accidentally annealed out during the preparation

Reproduced with permission of the copyright owner. Further reproduction prohibited without permission.

of the irradiated nickel samples. A comparison of the curve for 16% deformed Ni with that for high-dose irradiated Ni is shown in Fig. XII.

Owing to the precision of our positron annihilation angular correlation experiments, the difference between the angular correlation curves for two nickel samples annealed at 1150°C, as shown in Fig. XIII, is difficult to explain. It seems fairly obvious that something about the preparation of these two samples was different, but to the best of our knowledge they were both treated in the same manner.

Plastic Deformation in Metals

The deformation of a solid under the action of a finite minimum stress, the yield stress, is called "plastic" if after the removal of the stress a permanent deformation remains. Below this yield stress the deformation is elastic or anelastic. In other words, after removing the load the solid returns to its original shape either immediately (elastic) or gradually (anelastic).

A solid possessing a finite yield stress is "ductile" if it will undergo appreciable plastic deformation. If further deformation takes place under constant stress, the solid is said to deform in a "quasi-viscous" manner. In such a case the structure undergoes

Reproduced with permission of the copyright owner. Further reproduction prohibited without permission.

a plastic deformation, but it does not fail.

The point defects produced in plastically deformed f.c.c. metals are predominantly vacancies (29). Various mechanisms have been proposed for point defect formation during plastic deformation (29, 30). Vacancies can arise either by the movement of two edge dislocations past each other or by the movement of edge or screw dislocations with jogs. In the first case the intersection of every edge dislocation pair leads to the formation of a line of vacancies. Dislocations with jogs are necessary for the second case of point defect formation. The most important means of jog production involves the intersection of screw dislocations.

There is no doubt that point defects are produced during plastic deformation, but the number of vacancies or the distribution of vacancies produced by these mechanisms is not known so far with any certainty. Furthermore, because dislocations and defects can interact, the large number of dislocations introduced by plastic deformation complicates the interpretation of experiments.

Electron Irradiation Damage in Metals

High energy electron bombardment of a metal results in the production of vacancy-interstitial pairs (Frenkel defects). Assume that each atom in the solid is held in

Reproduced with permission of the copyright owner. Further reproduction prohibited without permission.

a potential well of depth E_d with a step-like boundary. Electrons with energies in the vicinity of 1 MeV have momenta close to the threshold value which is needed for transferring E_d (which is 24 eV for Ni or Fe) to typical atoms in the most favorable collisions. Electron bombardment produces the simplest type of displacement pattern, consisting primarily of isolated vacancy-interstitial pairs more or less randomly distributed. At room temperature (30°C), most interstitials migrate out because of the very low migration energy involved (about 0.1 eV).

It is well known that the average number of atoms displaced per unit volume is directly proportional to the time of bombardment. Thus one can expect a higher concentration of vacancies the longer a metal is irradiated.

Annealing

The annealing of damaged crystals results in the disappearance of vacancies through two processes, recrystallization and recovery. The process of recrystallization, which can be viewed as a transition from a thermodynamically unstable phase to a stable one, is accompanied by a complete change in the crystalline texture of the material. Evidently the damaged metal is unstable

Reproduced with permission of the copyright owner. Further reproduction prohibited without permission.

relative to the undamaged metal at all temperatures so that the transformation should take place at a finite rate in the course of time at any temperature above absolute zero. Since the process requires nucleation and growth of nuclei, and therefore requires thermal fluctuations, the rate of recrystallization will be extremely low at very low temperatures. It is emphasized that the lowest temperature at which recrystallization can occur depends principally on the degree of damage and the length of time the specimen is held at that temperature.

Recovery is the process by which the effects of damage are partly or fully removed by heating without recrystallization. It is found to occur most rapidly at temperatures just below the recrystallization temperatures and to decrease rapidly with decreasing temperature. It is reasonable to suppose that recovery is the more rapid process below the recrystallization temperature, whereas recrystallization is more rapid above it.

Reproduced with permission of the copyright owner. Further reproduction prohibited without permission.

CHAPTER V

CONCLUSIONS

The most interesting phenomenon from this work is the appreciable narrowing of the angular distribution curve observed for the damaged specimen compared to that obtained from the annealed (undamaged) specimen or the same specimen after annealing at 400°C. This feature, combined with the observations (16, 31) of the increased annihilation lifetime, inclines us to believe that the positrons tend to annihilate in the lower electron density regions at vacancies. Our results indicate that the angular correlation curve for 16% plastically deformed Ni annealed at 400°C is similar to that obtained for the undamaged specimen. Also, no change between either high-dose irradiated or 16% deformed Ni and Ni annealed near 100°C or 250°C for one hour was observed. Therefore, the results of this work are consistent with the interpretation that vacancies are responsible for the changes in angular correlation of positron annihilation curves in various damaged metals and alloys (15, 17, 18, 19).

Our results also indicate that either the concentration of vacancies saturates in plastic deformation or

Reproduced with permission of the copyright owner. Further reproduction prohibited without permission.

sufficient vacancies are present to saturate the effect on angular correlation distributions.

From the study presented, it may be seen that the angular correlation technique may be an effective tool for irradiation or deformation damage studies of metals.

Since changes in the angular correlation for both Fe (present work) and Pt (26) follow irradiation by electrons, it is disappointing that the irradiated Ni samples show no such change. Additional experiments on irradiated Ni are being planned; it seems likely that eventually angular correlation results qualitatively similar to those for Fe and Pt will be obtained when the techniques of irradiation are improved.

However, the angular correlation distributions are sensitive to details of the product of positron and electron wave functions, and hence it seems likely that the aim of theoretical work will be able to reproduce both the experimental angular correlation curves and the total annihilation rate for the damaged metals. Experimentally, careful lifetime measurements in the damaged metals are necessary in order to observe possible variation of lifetime with the density of electrons, and the correlation between the lifetime and the narrowing angular distribution should be further investigated in order to understand in more detail the nature of the positron annihilation mechanism.

Reproduced with permission of the copyright owner. Further reproduction prohibited without permission.

BIBLIOGRAPHY

(1) DeBenedetti *et al.*, "On the Angular Distribution of Two-Photon Annihilation Radiation." Physical Review, LXXVII, 205 (1950).

(2) S. Berko, and F. L. Hereford, "Experimental Studies of Positron Interactions in Solids and Liquids." Review of Modern Physics, XXVIII, 299 (1956).

(3) A. T. Stewart, "Momentum Distribution of Metallic Electrons by Positron Annihilation." Canadian Journal of Physics, XXXV, 168 (1957).

(4) P. R. Wallace, "Positron Annihilation in Solids and Liquids." Solid State Physics, X, 1 (1960).

(5) A. T. Stewart, J. H. Kusmiss, and R. H. March, "Electrons in Liquid Metals by Positron Annihilation." Physical Review, CXXXII, 495 (1963).

(6) J. H. Kusmiss, "Positron Annihilation in Solid and Liquid Metals and Semiconductors." Unpublished Doctor's Thesis, University of North Carolina, Chapel Hill, North Carolina, 1965.

(7) A. T. Stewart, and J. B. Shand, "Motion of Positrons in Sodium." Bulletin of American Physics Society, X, 21 (1965).

(8) L. G. Lang, and N. C. Hien, "Electron Momentum Distributions in Single-Crystal C_d." Physical Review, CX, 1062 (1958).

(9) S. Berko, and J. S. Plaskett, "Correlation of Annihilation Radiation in Oriented Single Metal Crystals." Physical Review, CXII, 1877 (1958).

(10) Chanchal K. Majumdar, "Two Contributions to the Theory of Annihilation of Positrons in Metals." Physical Review, CXL, A227 (1965).

(11) L. G. Lang, and S. DeBenedetti, "Angular Correlation of Annihilation Radiation in Various Substances." Physical Review, CVIII, 914 (1957).

Reproduced with permission of the copyright owner. Further reproduction prohibited without permission.

(12) Berko, Kelly, and Plaskett, "Angular Correlation of Annihilation Radiation from Oriented Graphite." Physical Review, CVI, 824 (1957).

(13) A. T. Stewart, J. B. Shand, J. J. Donaghy, and J. H. Kusmiss, "Fermi Surface of Beryllium by Positron Annihilation." Physical Review, CXXVIII, 118 (1962); J. J. Donaghy, and A. T. Stewart, "Positron Annihilation in Sodium Single Crystals." Bulletin of American Physics Society IX, 238 (1964).

(14) D. R. Gustafson, and A. R. McKintosh, "Positron Annihilation in Rare-Earth Metals." Journal of Physical Chemistry Solid, XXV, 389 (1964).

(15) S. Berko, and J. C. Erskine, "Angular Distribution of Annihilation Radiation from Plastically Deformed Aluminium." Physical Review Letters, XIX, 307 (1967).

(16) I. K. MacKenzie et al., "Temperature Dependence of Positron Mean Lives in Metals." Physical Review Letters, XIX, 946 (1967).

(17) Ya. Dekhtyar, D. A. Levina, and V. S. Mikhalenkov, "Electron-Positron Annihilation in Plastically Deformed Metals." Doklady Akad. Nauk SSSR CLVI, 795 (1964), (translation: Soviet Physics -- Doklady IX, 492 (1964)).

(18) Ya. Dekhtyar, V. S. Mikhalenkov, and S. G. Sakharova, "Annihilation of Positrons by Electrons in Plastically Deformed Metals having a B.C.C. Lattice." Doklady Akad. Nauk SSSR CLXVIII, 785 (1966), (translation: Soviet Physics -- Doklady XI, 537 (1966)).

(19) S. M. Kim, and A. T. Stewart (private communication).

(20) G. E. Lee-Whiting, "X-ray Absorption Line-Width and Electron Stopping Power Calculated with a Screened Coulomb Interaction." Process Royal Society A212, 362 (1952); "Thermalization of Positrons in Metals." Physical Review, XCVII, 1557 (1955).

(21) D. Bohm, and D. Pines, "A Collective Description of Electron Interactions: III. Coulomb Interactions in a Degenerate Electron Gas." Physical Review, XCII, 609 (1953).

Reproduced with permission of the copyright owner. Further reproduction prohibited without permission.

(22) R. E. Bell and R. L. Graham, "Time Distribution of Positron Annihilation in Liquids and Solids." Physical Review, XC, 644 (1953).

(23) R. A. Ferrell, "A Theory of Positron Annihilation in Solids." Review Modern Physics, XXVIII, 308 (1956).

(24) J. M. Jauch and F. Rohrlich, The Theory of Photons and Electrons. New York: Addison-Wesley Publishing Co., Inc., 1959.

(25) K. L. Rose and S. DeBenedetti, "Positron Annihilation in Solid Argon." Physical Review, CXXXVIII, A927 (1965).

(26) J. H. Kusmiss (private communication).

(27) Sosin et al., "Electrical Resistivity Recovery in Cold-Worked and Electron-Irradiated Nickel." Acta Metallurgica, VII, 478-494 (1959).

(28) A. H. Cottrell, Vacancies and other defects in Metals. London: Institute of Metals, London, 1958.

(29) A. C. Damask, G. J. Dienes, Point Defects in Metals, New York: Gordon and Breach Science Publishers, 1963.

(30) N. F. Mott, "Recent Advances in the Electron Theory of Metals." Philosophical Magazine, XLIII, 1151 (1952); "A Theory of Work-Harding of Metals: II. Flow without Slip-Lines, Recovery and Creep." Philosophical Magazine, XLIV, 741 (1953).

(31) J. C. Grosskreutz, and W. E. Millett, "Measurements of Positron Lifetimes in Cyclically Deformed Al and Cu." Physical Letters, 28A, 621 (1969).

Reproduced with permission of the copyright owner. Further reproduction prohibited without permission.